

Supporting Information for

**Versatile NiO/mesoporous carbon nanodisks: Controlled synthesis from hexagon
shaped heterobimetallic metal-organic frameworks**

Dehong Zeng¹, Ying Yang^{1,*}, Feng Yang, Fangmin Guo, Senjie Yang,

Baijun Liu*, Shijie Hao, and Yang Ren

Email: catalyticsscience@163.com

S1 Experimental

S1.1 Materials

All the reagents used were of analytical grade, and were used without further treatment. Zinc acetate dihydrate ($\text{Zn}(\text{Ac})_2 \cdot 2\text{H}_2\text{O}$), Nickel acetate tetrahydrate ($\text{Ni}(\text{Ac})_2 \cdot 4\text{H}_2\text{O}$), 4-nitrophenol, sodium borohydride and N,N-dimethylformamide (DMF) were obtained from Sinopharm Chemical Reagent. Trimesic acid (H_3BTC) was purchased from Shanghai TCI Chemical Industry Development Co., Ltd. Polytetrafluoroethylene (PTFE, 60 wt%) and acetylene black was purchased from Shanghai Macklin Biochemical Co., Ltd. Nitrogen was supplied by Beijing Beiwen Special Gases Factory.

S1.2 Synthesis of NiO/mesoporous carbon nanodisk

$\text{Zn}(\text{Ac})_2 \cdot 2\text{H}_2\text{O}$, $\text{Ni}(\text{Ac})_2 \cdot 4\text{H}_2\text{O}$ and H_3BTC were used as the precursors for zinc-nickel-trimesic acid metal-organic framework disk synthesis. The molar ratio of precursors used in the preferred preparation is 6 H_3BTC : 5 Metal ($\text{Ni}_x\text{Zn}_{1-x}$): 650 DMF, where x was defined as the $\text{Ni}/(\text{Zn}+\text{Ni})$ molar ratio in the synthetic mixture, and was set to be 0, 0.3, 0.5, 1.0, 10.0, 50.0 and 80.0%. Typically, certain amount of metal salts combined with 1.25 g of H_3BTC was dissolved in 50 mL of DMF under constant agitation at room temperature for a certain duration. The resulting mixture was filtered and washed with DMF and the precipitate was dried at 80 °C for 5 h. Then, the precipitate were directly carbonized with a heating rate of 5 °C min^{-1} up to 910 °C and kept at this temperature for 2 h, yielding NiO/MCN- x .

S1.3 Characterization

The morphology of the samples was characterized by scanning electron microscopy (SEM, FEI-Quanta 200F) and transmission electron microscopy (TEM, FEI Tecnai G2 F20). Samples for TEM observation were prepared by drying a drop of sample powder ethanol suspension on a holey carbon microgrid supported on a 300 mesh copper grid. The phases of the samples were examined by X-ray diffraction (XRD) analysis (Bruker D8). The infrared spectra of the samples were recorded in KBr disks using a Nicolet Nexus 870 FTIR spectrometer. Thermogravimetric analysis (TGA) was performed from room temperature to 950 °C in N₂ atmosphere using an STA 449F5 Jupiter thermogravimetric analyzer (NETZSCH) at a heating rate of 10 °C per minute. The Raman spectra were recorded using a HORIBA Jobin Yvon HR800 instrument with an excitation wavelength of 633 nm. X-ray photoelectron spectroscopy (XPS, K-Alpha1063) were applied to determine the chemical compositions of the samples. The nitrogen adsorption-desorption isotherms of the samples were measured by using a Micrometrics KuboX 1000 porosimeter at 77 K, and the specific surface area and mesopore size distribution were calculated using the BET and BJH methods. Raman spectra were recorded with a HORIBA Jobin Yvon HR800 with a microscope attachment. The laser wavelength of 633 nm was focused using a diffraction limited spot, and the scan time was 2 s for each sample. High-energy X-rays of 115 KeV energy and 0.6 mm × 0.6 mm beam size were used to obtain two-dimensional (2D) diffraction patterns in the transmission geometry using a Perkin-Elmer large area detector placed at 1.6 m from the sample.

In situ synchrotron HE-XRD: The *in situ* synchrotron XRD data for the phase

change during the transformation of Ni-ZnBTC-0.5% to NiO/MCN-0.5% were collected at Beamline 11-ID-C ($\lambda = 0.1173 \text{ \AA}$) of the Advanced Photon Source, using an image plate detector in the transmission mode. Mylar film was used as window to allow the penetration of synchrotron beam in the present *in situ* cell. The *in situ* cell was assembled with Ar atmosphere and circulation water, and heated up to 930 °C at a rate of 5 ° min⁻¹. The phase analysis of the XRD peak profile was done by comparison with the standard JCPDS index.

The Ni dosage was estimated by inductively coupled plasma-atomic emission spectroscopy (ICP-AES) analysis conducted on a Perkin Elmer emission spectrometer. Certain amount of vacuum-dried sample was placed in a crucible and heated at 550 °C for 2 h in air. The residue was then dissolved in 3 mL of aqua fortis solution, and each solution was filtered through a 0.45 μm polyethersulfone filter and set the constant volume to be 10 mL, and then submitted for analysis.

S1.4 Electrochemical test

Electrochemical experiments were carried out in a three-electrode system with an electrochemical workstation (CHI 660E, CH Instruments, Inc.). The working electrodes were prepared by mixing the NiO/carbon hexagonal nanodisk composites (70 wt%), carbon black (20 wt%) and polytetrafluoroethylene (10 wt%). Then the paste was pressed at Ni foam (1 cm \times 1 cm) and then dried at 80 °C for 5 hours. The mass of electroactive materials in the electrode is 0.7 mg for all of the samples tested. The Hg/HgO electrode was used as a reference electrode, and Pt wire as a counter electrode. The cyclic voltammetry curves were measured in a potential range between

-1.0 and 0 V at different scan rates, and the charge/discharge processes were performed by cycling the potential from -1.0 to 0 V at different current densities in 6 M KOH aqueous electrolyte. Electrochemical impedance spectroscopy (EIS) tests were performed using a sinusoidal signal with mean voltage of 0 V and amplitude of 10 mV over a frequency range of 1 MHz to 0.01 Hz. The cyclic stability was evaluated by charge/discharge measurements at a current density of 5 A g⁻¹.

The electrochemical gravimetric specific capacitance of the electrode material based on GCD curves was determined as follows:

$$C_n = \frac{C}{m} = \frac{I \times \Delta t}{m \times \Delta V}$$

in which C_n is the gravimetric specific capacitance (F g⁻¹), C is the capacitance (F), m is the mass of electrode material (g), I is the charge-discharge current (A), Δt is the discharge time (s), and ΔV is the potential window of charge-discharge (V).

S1.5 Catalytic property

The reduction of 4-NP was carried out in a quartz cuvette and monitored by using a UV-vis spectroscopy (754PC) at room temperature. A total of 25 μ L of aqueous 4-NP solution (0.01 M) was mixed with 2.5 mL of fresh NaBH₄ (0.01 M) solution. Subsequently, a given amount of nickel catalyst was added to start the reaction, and the UV spectrometry was employed to monitor the reduction by measuring the absorbance of the solution at 400 nm as a function of time. The solution was *in situ* measured at certain intervals to obtain the successive information about the reaction. After the reaction was finished, the catalyst was quickly separated, rinsed with water and re-dispersed into the mixture of new reactants to initiate another reaction cycle.

Table S1 Crystallite size, Ni and NiO content in different NiO/MCN composites

Materials	Ni/(Zn+Ni) feed ratio (%)	Average crystallite size ^a (nm)	Ni content ^b (wt%)	NiO content (wt%)
NiO/MCN-0.3%	0.3	51.5	0.30	0.38
NiO/MCN-0.5%	0.5	69.7	0.84	1.07
NiO/MCN-1.0%	1.0	52.7	2.61	3.32

^aCalculated by Debye-Scherrer equation: $L = K\lambda/d(\theta)\cos\theta$, in which K is the crystallite shape factor (0.96), λ is the wavelength of the radiation used (0.1173 Å), θ is the Bragg diffraction angle, and $d(\theta)$ is the full width at half maximum. In this study, the $d(\theta)$ is calibrated as the following methods: 1) Get the full-width at a half maximum of a peak, say it is $\Delta\theta$ for peak (111). 2) The instrument broadening is $\theta = 0.002$ degrees. 3) Corrected peak broadening $d(\theta) = (\Delta\theta^2 - \theta^2)^{1/2}$. 4) Change $d(\theta)$ from degree to radian: $\pi/180$. ^b Estimated by ICP-AES.

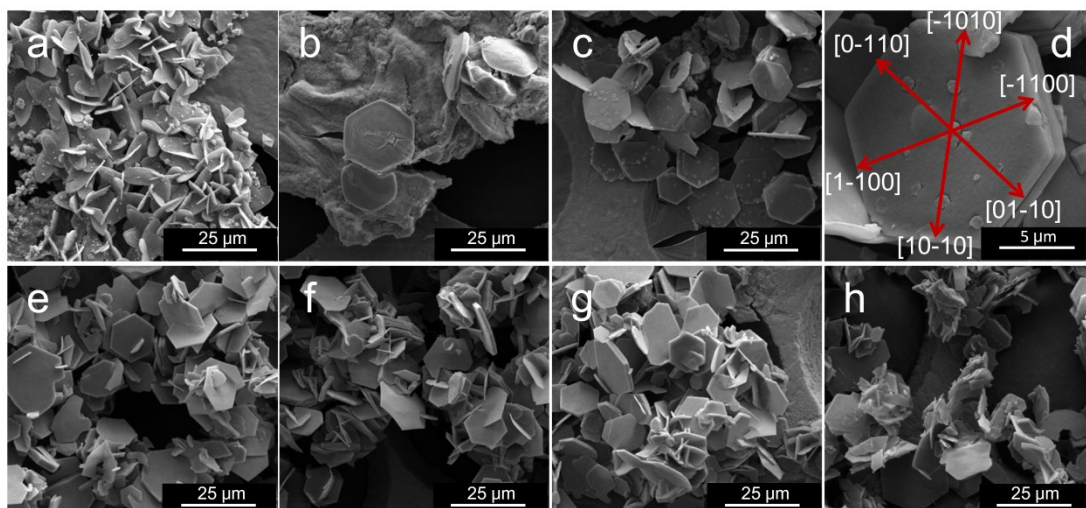


Fig. S1 SEM images of zinc-nickel-trimesic acid metal-organic framework synthesized at a different time: (a) 10 s, (b) 30 s, (c) 1 min, (d) 1 min (enlargement), (e) 5 min, (f) 10 min, (g) 30 min, and (h) 60 min.

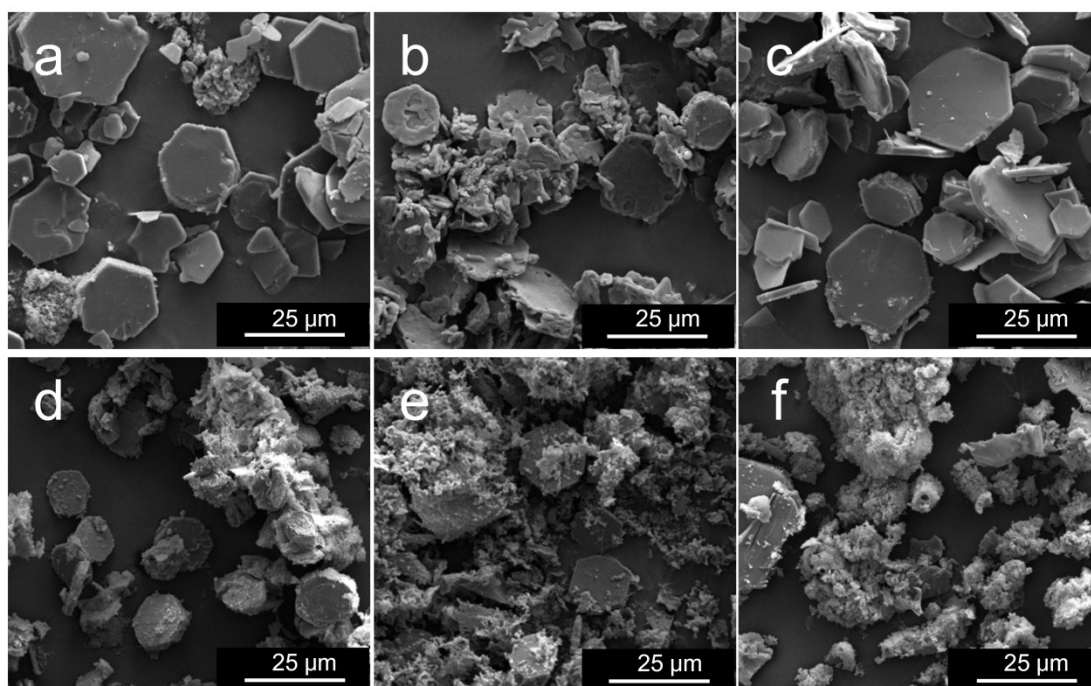


Fig. S2 SEM images of zinc-nickel-trimesic acid metal-organic framework synthesized within 1 min using different Ni/(Zn+Ni) feed ratios: (a) 0%, (b) 0.3%, (c) 1.0%, (d) 10.0%, (e) 50.0% and (f) 80.0%.

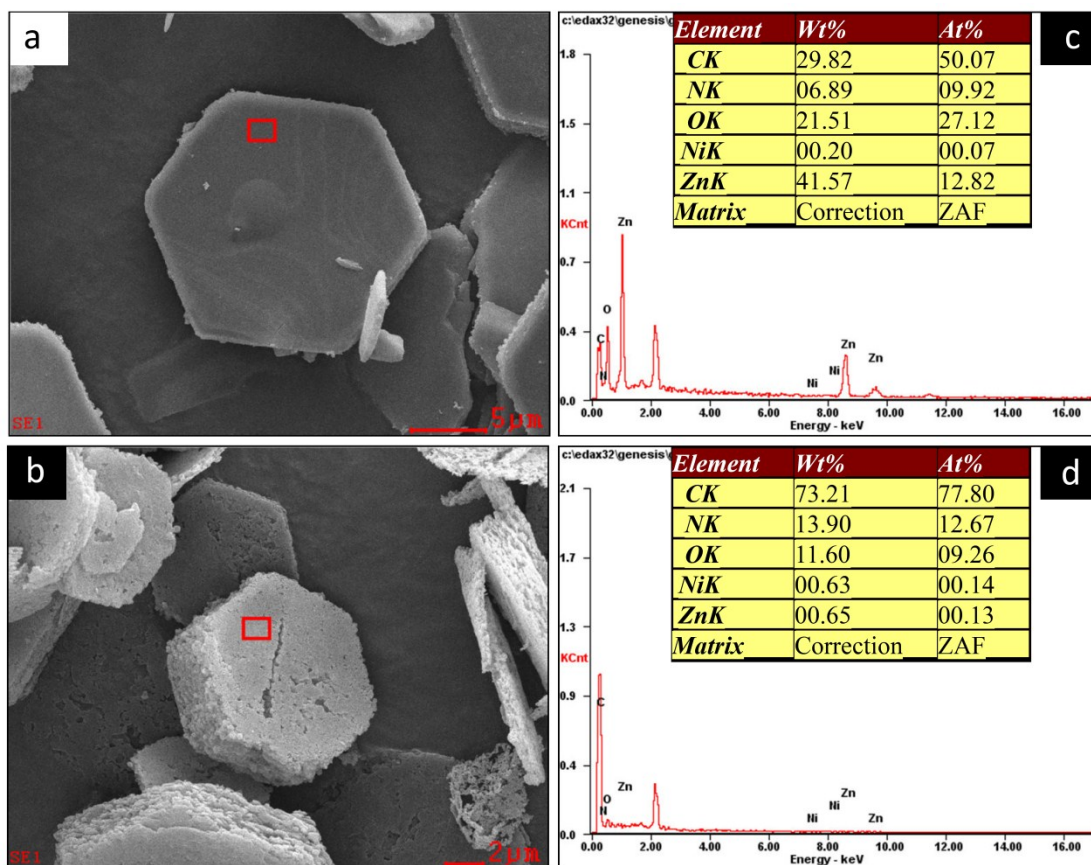


Fig. S3 SEM image (a,b) and the corresponding energy dispersive spectroscopy (c,d) of (a,c) Ni-ZnBTC-0.5% and (b,d) NiO/MCN-0.5%.

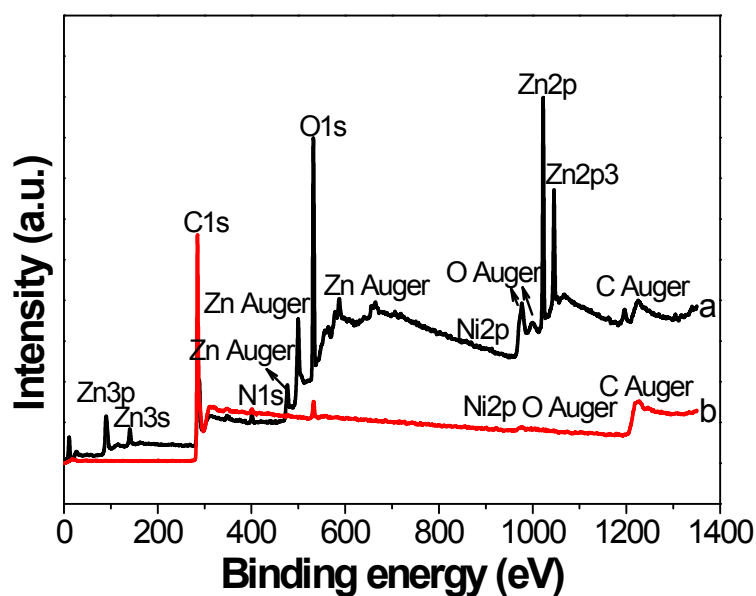


Fig. S4 XPS survey spectrum of (a) Ni-ZnBTC-0.5% and (b) NiO/MCN-0.5%.

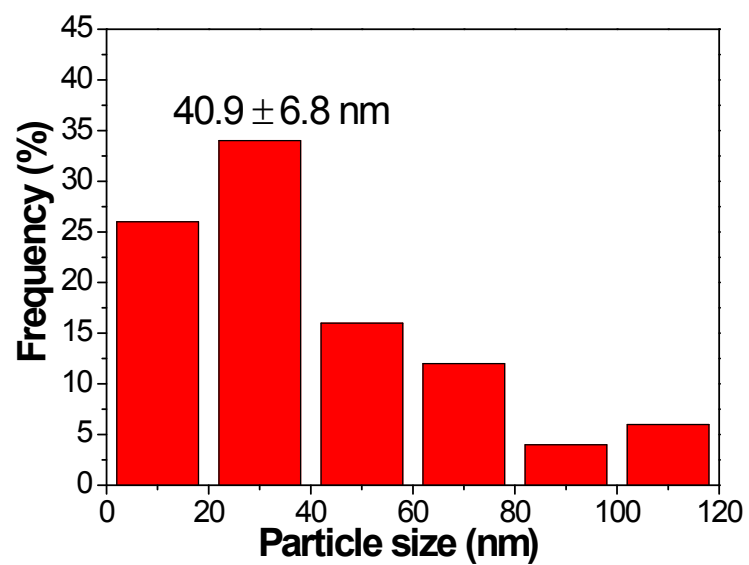


Fig. S5 Particle size distribution histogram for NiO/MCN-0.5%.

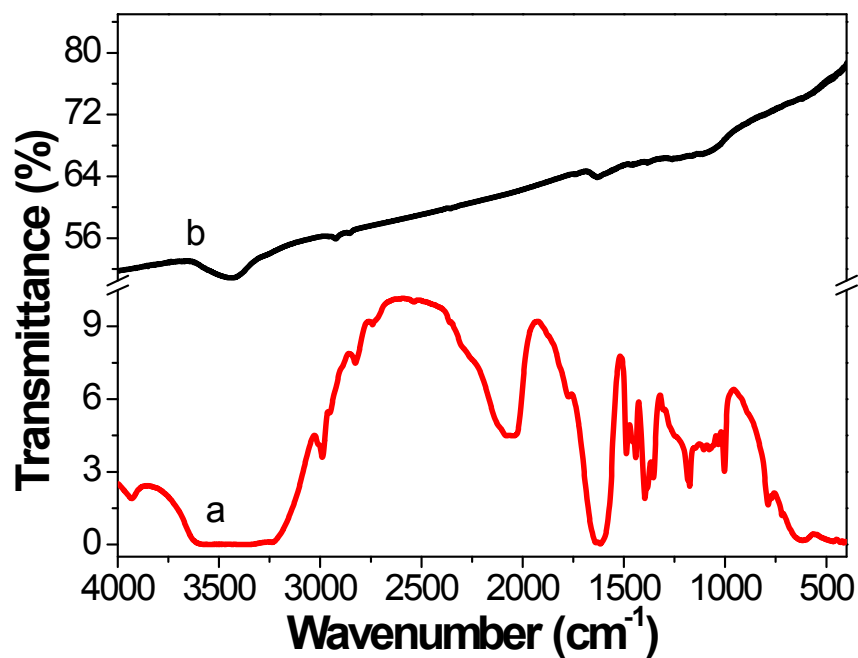


Fig. S6 FT-IR spectra of (a) Ni-ZnBTC-0.5% and (b) NiO/MCN-0.5%.

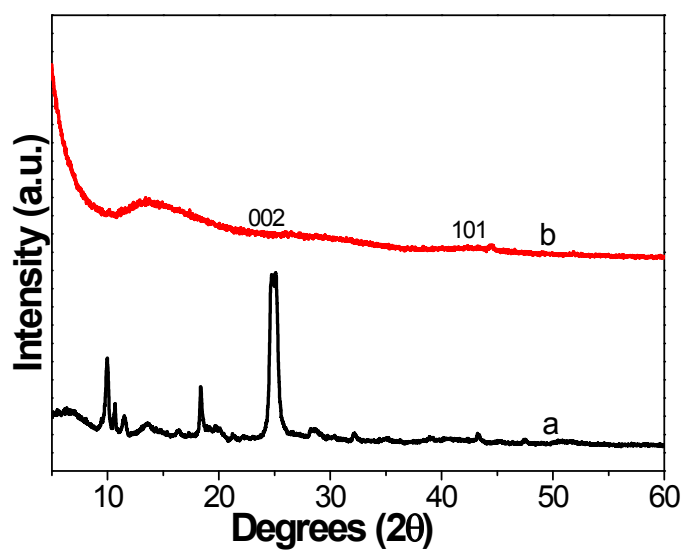
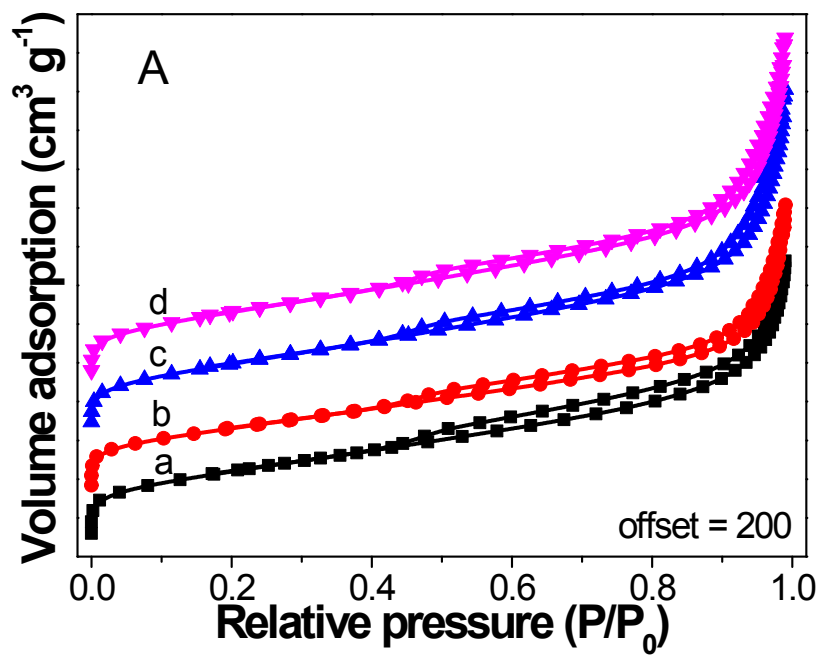


Fig. S7 XRD patterns of (a) Ni-ZnBTC-0.5% and (b) NiO/MCN-0.5%.



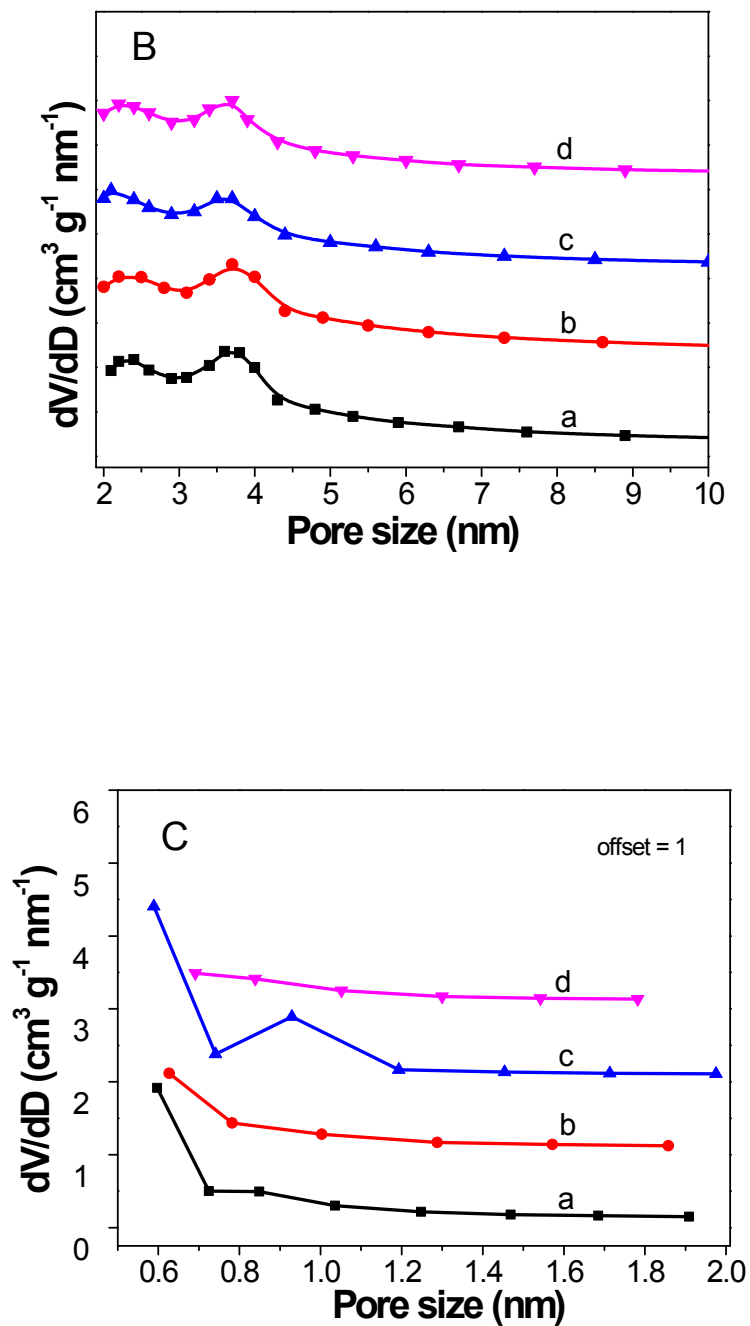
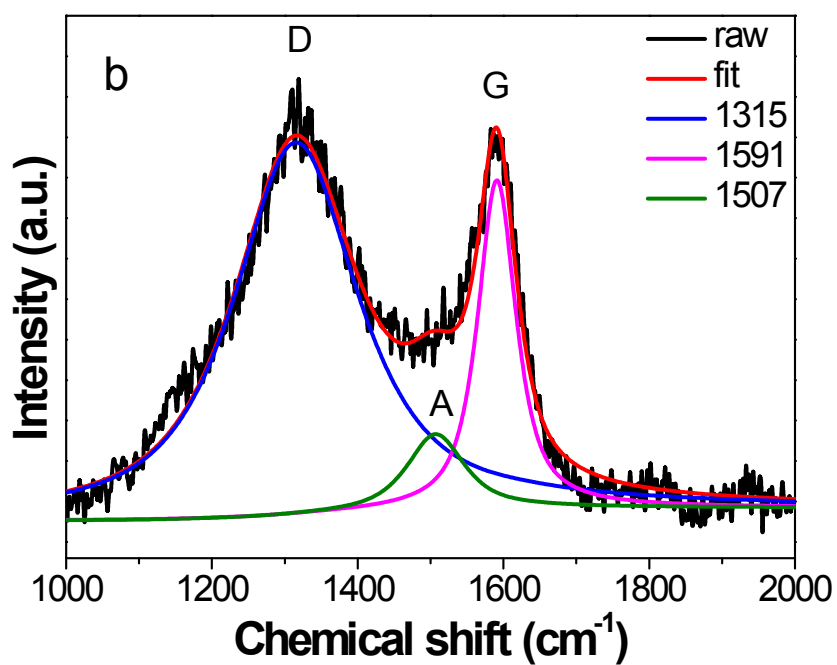
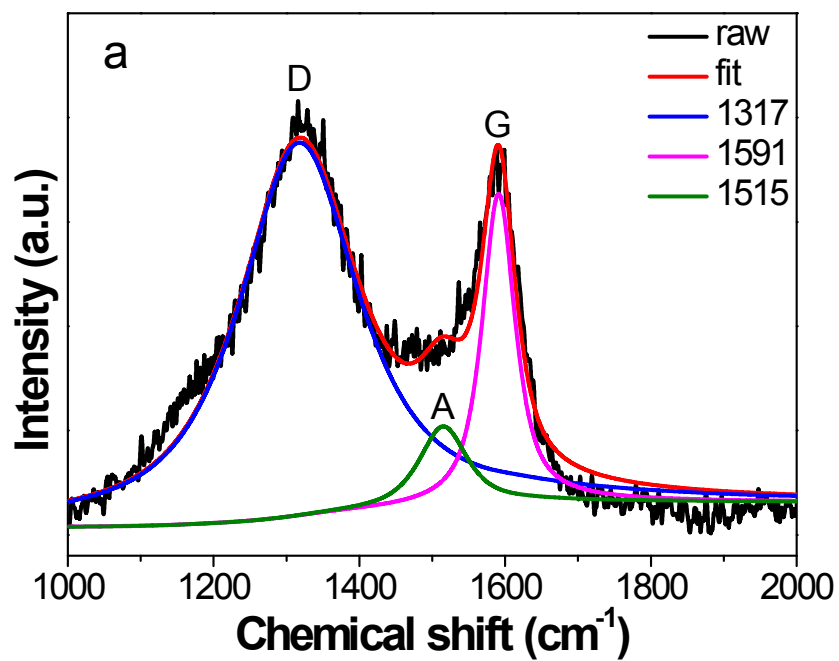


Fig. S8 N_2 adsorption-desorption isotherms (A) and the corresponding mesopore (B) and micropore size (C) distributions for (a) MCN, (b) NiO/MCN-0.3%, (c) NiO/MCN-0.5% and (d) NiO/MCN-1.0%.



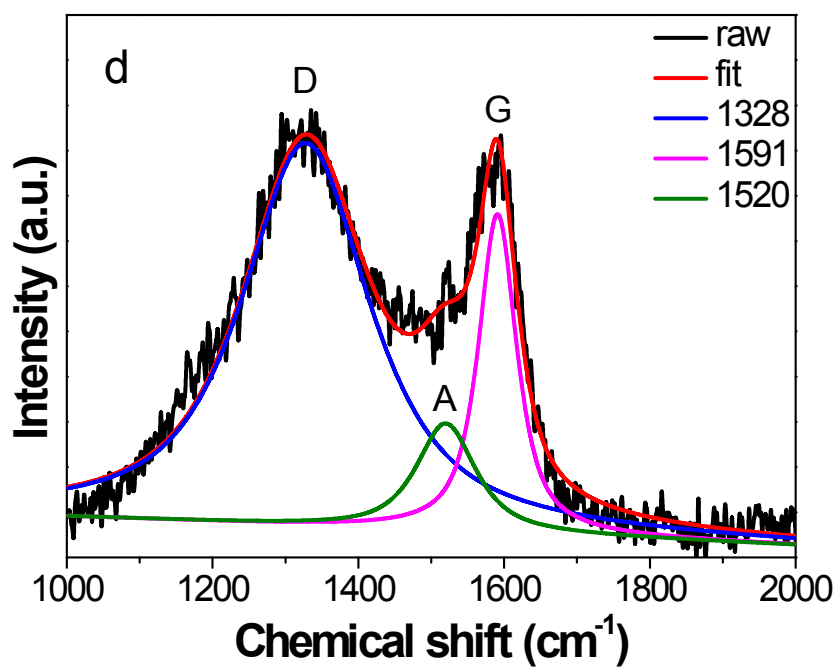
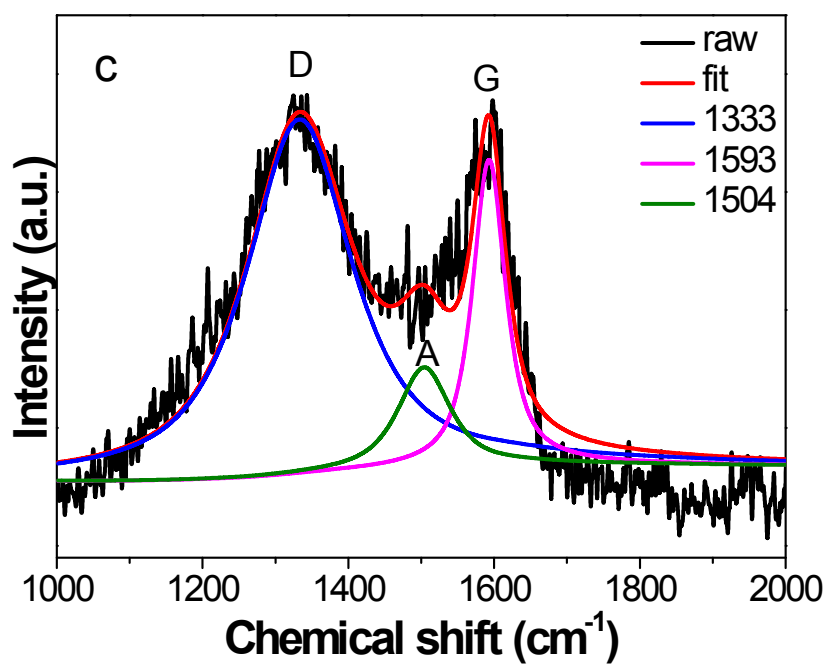


Fig. S9 Raman spectrum (a) MCN, (b) NiO/MCN-0.3%, (c) NiO/MCN-0.5% and (d) NiO/MCN-1.0%.

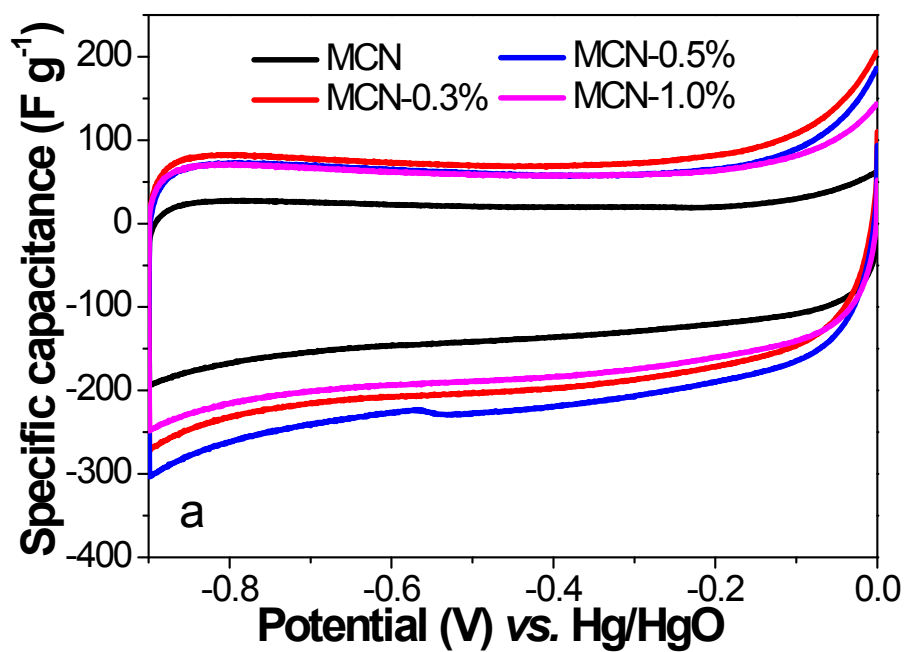
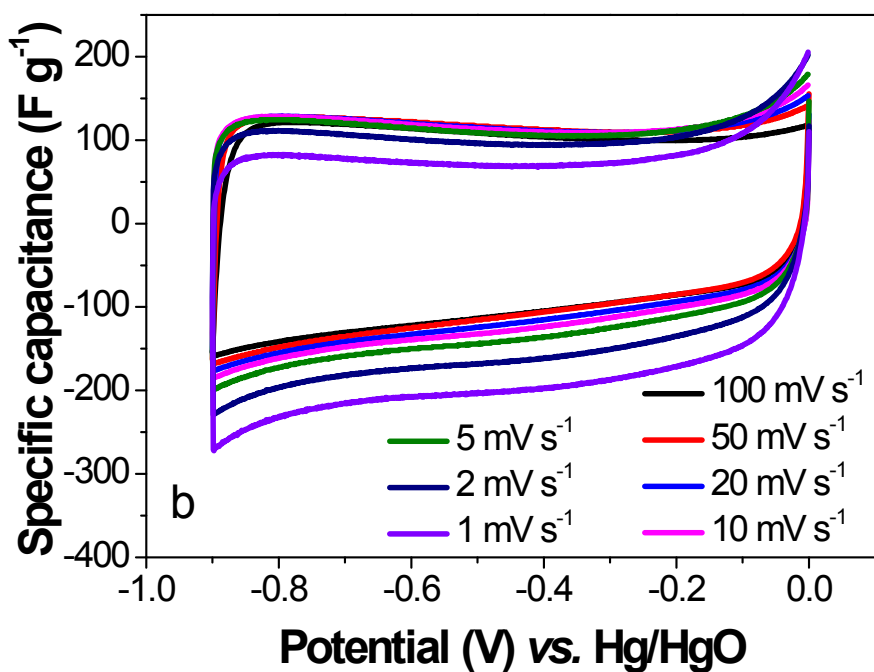


Fig. S10 CV curves at 1 mV s^{-1} for different samples.



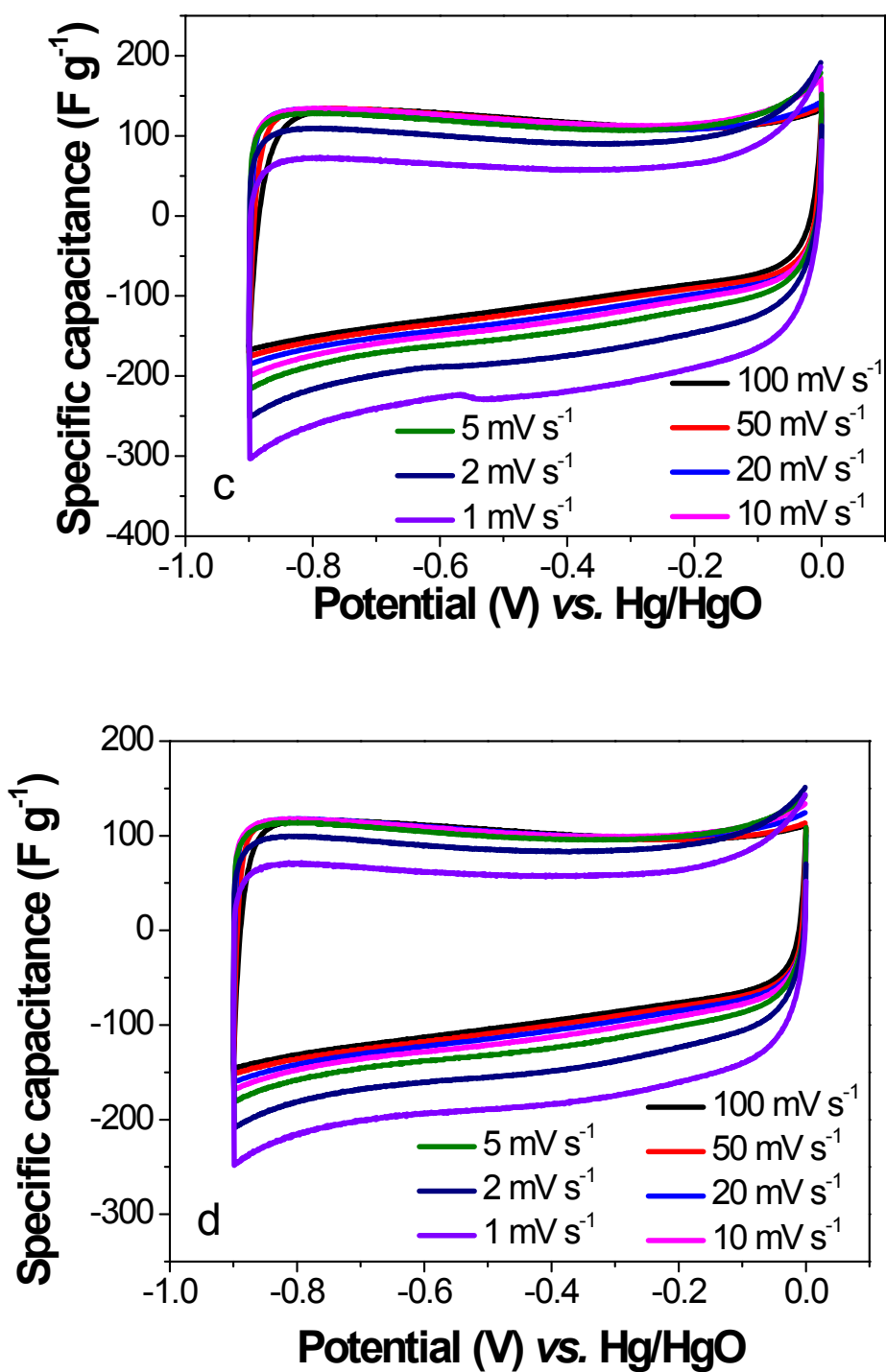
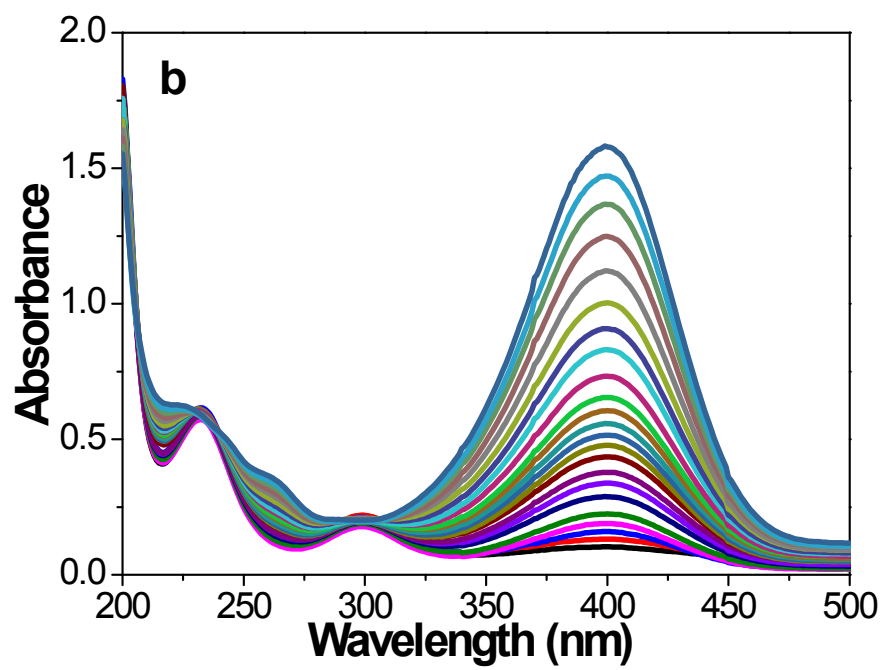
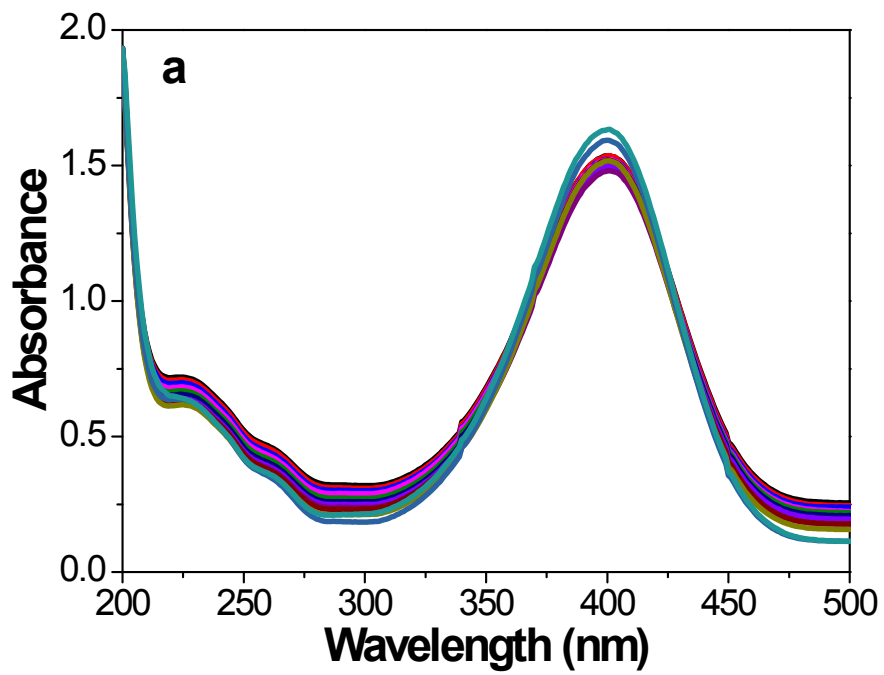
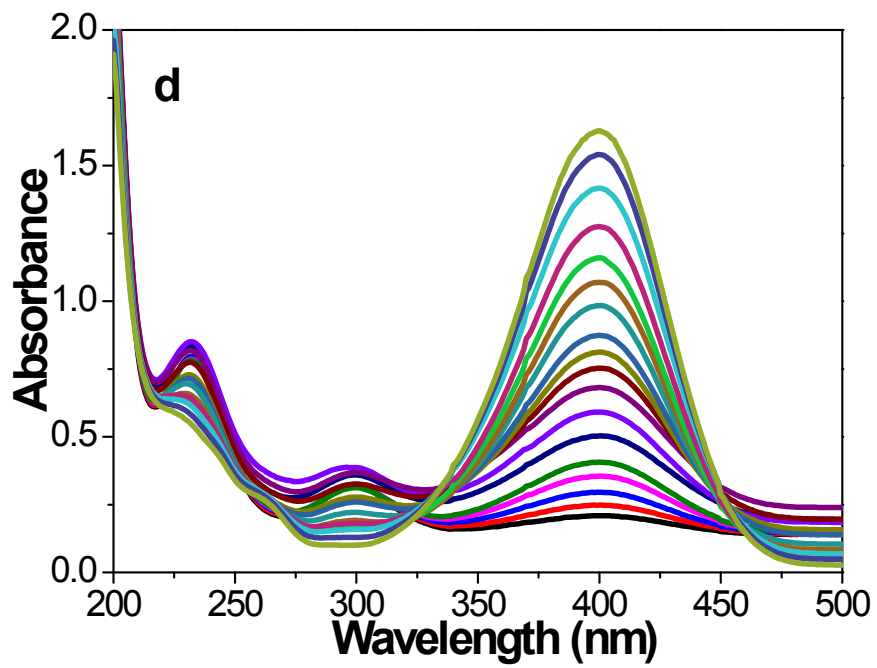
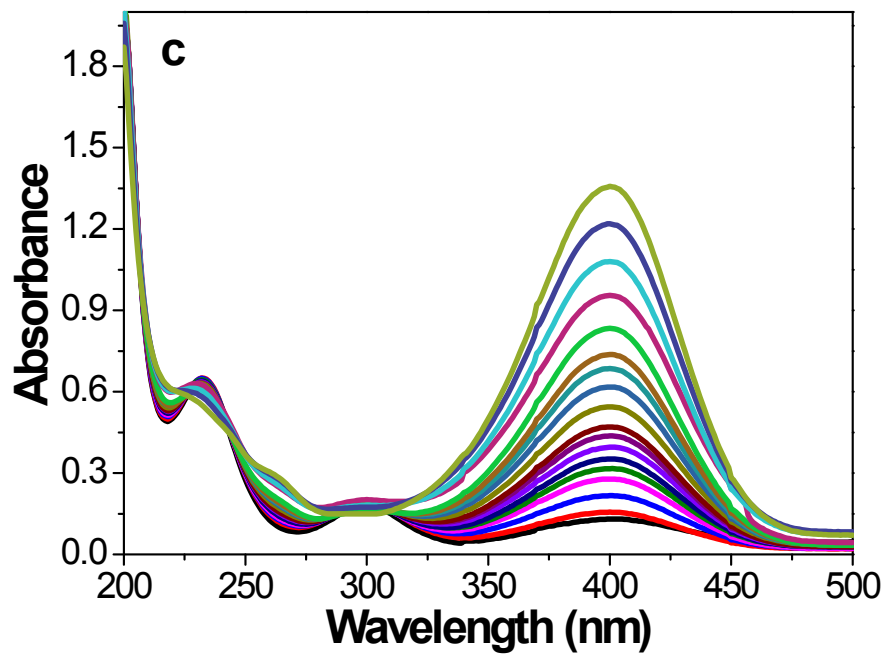


Fig. S11 CV curves at different scans for (a) MCN, (b) NiO/MCN-0.3%, (c) NiO/MCN-0.5% and (d) NiO/MCN-1.0%.





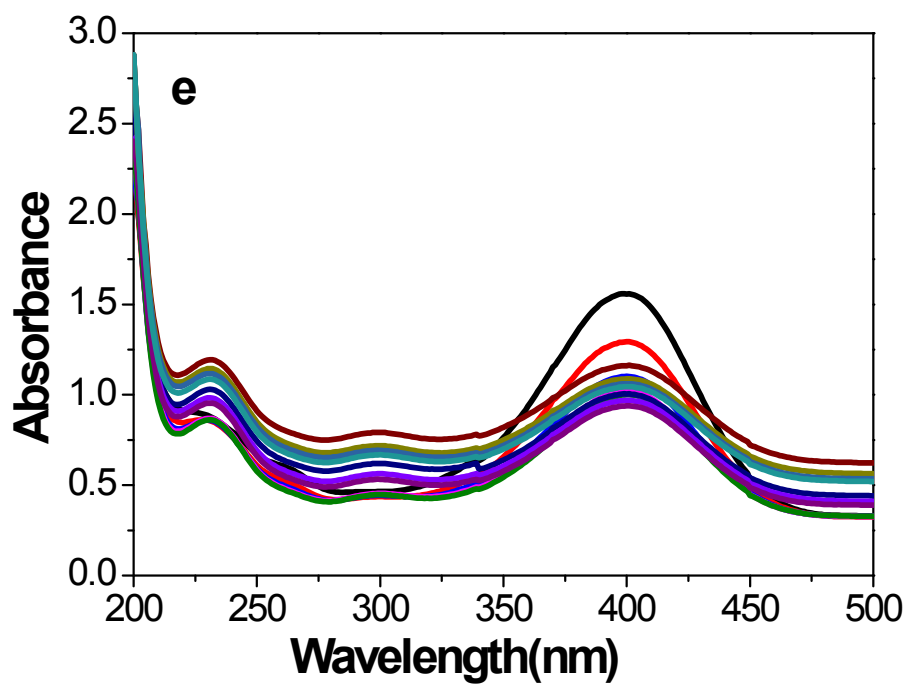


Fig. S12 The reduction of 4-NP in aqueous solution recorded every 2.8 min using (a) 1.0 mg MCN, (b) 0.8 mg NiO/MCN-0.3%, (c) 0.4 mg NiO/MCN-0.5%, (d) 0.3 mg NiO/MCN-1.0% and (e) 1.5 mg NiO/MCN-10.0%.